Journal of Cranio-Maxillo-Facial Surgery 47 (2019) 311–319

Contents lists available at ScienceDirect

Journal of Cranio-Maxillo-Facial Surgery

journal homepage: www.jcmfs.com

Quantitative assessment of symmetry recovery in navigation-assisted surgical reduction of zygomaticomaxillary complex fractures

Tingwei Bao [a], Di Yu [b], Qifeng Luo [c], Huiming Wang [a], Jianhua Liu [a], Huiyong Zhu [a, *]

[a] Department of Oral and Maxillofacial Surgery, The First Affiliated Hospital, School of Medicine, Zhejiang University, No. 79 Qingchun Road, Hangzhou, Zhejiang, 310003, China
[b] General Department, Hangzhou Dental Hospital, No. 1 Pinghai Road, Hangzhou, Zhejiang, 310001, China
[c] Department of Prosthodontics, Hangzhou Dental Hospital, No. 1 Pinghai Road, Hangzhou, Zhejiang, 310001, China

ARTICLE INFO

Article history:
Paper received 17 August 2018
Accepted 6 December 2018
Available online 12 December 2018

Keywords:
ZMC fracture
Navigation
Symmetry
Asymmetry index
Quantitative assessment

ABSTRACT

Purpose: To evaluate the effects of surgical navigation in zygomaticomaxillary complex (ZMC) fracture reduction. ZMC symmetry was assessed quantitatively.
Materials and methods: The sample comprised 25 patients who underwent surgical reduction of comminuted ZMC fractures. They were divided into two groups according to the use of surgical navigation. Reduction outcomes were evaluated using three-dimensional computed tomography models. Five pairs of landmarks were identified on all craniofacial models, and asymmetry scores were calculated based on their coordinates. In quantitative analyses, symmetry and orbital volume were compared between groups.
Results: All patients recovered uneventfully. Greater symmetry was observed in the navigation group than in the control group for three of the five pairs of landmarks ($p < 0.05$). Although postoperative volumes of the injured orbits were similar between the two groups ($p > 0.05$), reduced orbital volumes were larger in the navigation group, indicating better restoration of the fractured orbits ($p < 0.05$).
Conclusions: The use of surgical navigation can increase postoperative symmetry of the bilateral ZMC. The quantitative evaluation of clinical outcomes is precise and highly reliable.

1. Introduction

Zygomaticomaxillary complex (ZMC) fractures occur frequently because of the prominent midface position of the ZMC (Ozyazgan et al., 2007; Salentijn et al., 2013); they comprise up to 40% of all facial fractures (Bogusiak and Arkuszewski, 2010; Marinho and Freire-Maia, 2013). Facial asymmetry is a common complaint in patients with ZMC fractures.

The surgical treatment of ZMC fractures involves reduction and internal fixation. Anatomical reduction may be difficult to achieve, especially in the case of comminuted fracture, because of the complex shape of the ZMC. The challenge is related to the intraoperative confirmation of correct bone position. Traditionally, the reduction of a ZMC fracture was verified intraoperatively by tactile and direct visualization. However, clinical evaluation can be hampered by swelling. Without accurate intraoperative measurement, satisfactory midface symmetry is difficult to obtain.

Computer-assisted navigation systems (CANSs) allow the real-time visualization of operative sites and comparison with patient images without the need for additional radiation. Lübbers et al. (2011) proposed the use of CANS-assisted surgery in the treatment of severe unilateral midface fractures. Previous studies have focused on navigation methods and ways to improve CANS applications. The proper utilization of CANSs is expected to increase the accuracy of ZMC fracture reduction. The surgical outcome is usually assessed primarily by observation of the aesthetic outcome (i.e., restoration of facial symmetry) and secondarily by radiographic imaging. Quantitative evaluation of the surgical outcome remains controversial, although a quantitative approach is essential for preoperative planning and postoperative assessment.

Several techniques have been developed for the assessment of ZMC symmetry and operative errors. Chromatography is commonly used to reveal differences between postoperative computed tomography (CT) data and virtual plans (He et al., 2013). Different

* Corresponding author.
E-mail address: zhuhuiyong@zju.edu.cn (H. Zhu).

https://doi.org/10.1016/j.jcms.2018.12.003
1010-5182/

colors represent different degrees of error, creating an easy-to-read image. Imaging-based measurement using the ZMC eminence has been described, but it cannot be applied in cases of complex fracture of the zygoma with dislocation of the summit (Lerhe et al., 2017). Landmark-based imaging analysis can provide more detailed information, and is suitable for statistical analyses. The degree of ZMC symmetry can be calculated using appropriate formulas (Belcastro et al., 2016).

The goal of this study was to quantitatively analyze the surgical results through the computation of asymmetry scores and measurement of orbital volumes. The value of CANS used in the reduction of ZMC fracture is highlighted.

2. Materials and methods

This retrospective study involved the review of 25 consecutive cases of comminuted ZMC fracture treated in the Oral and Maxillofacial Surgery Department of the First Affiliated Hospital of Zhejiang University between April 2012 and November 2016. This study was approved by the Ethics Committee of Institution Research of the First Affiliated Hospital, School of Medicine, Zhejiang University. Additionally, written informed consent was obtained from all the patients.

The inclusion criteria were: age >18 years, unilateral comminuted ZMC fracture (occurring within 2 weeks of admission), and visually apparent asymmetry of the midface caused by bone displacement. The fractures of the skull bases and craniofacial anomalies were excluded, which can potentially hamper confirmation along the median sagittal plane.

In total, 17 male and 8 female patients, with a mean age of 40.4 ± 11.36 years, were included in this study. The patients were divided into two groups according to the type of surgery. In the navigation group (10 men, 5 women; mean age, 41.06 ± 11.78 years), fracture reduction was assisted by real-time surgical navigation. In the control group (7 men, 3 women; mean age, 39.4 ± 10.62 years), the operations were performed based on the surgeon's clinical experience, without navigation.

All patients underwent preoperative and postoperative spiral CT of the skull (0.67-mm slices). The surgical navigation system consisted of iPlan 3.0 software (BrainLAB, Feldkirchen, Germany) and a navigation workstation. The iPlan software was used for virtual planning and analysis for all patients.

2.1. Virtual planning

A single surgeon (T. B) performed all of the virtual planning. CT data in Digital Imaging and Communications in Medicine (DICOM) format were imported into the iPlan software for surgical planning. According to the protocol, the median sagittal plane was delineated perpendicular to the Frankfort horizontal (FH) plane, passing through the middle of the sella turcica and nasion. It was defined as the reference plane for the restoration of facial symmetry by mirroring of the unaffected contralateral bones. Different colors were applied to highlight differences between mirror images and fracture images (Fig. 1). For the navigation group, CT data and virtual planning models were then transferred to the intraoperative navigation workstation.

2.2. Surgical techniques

The surgeries were performed under general anesthesia. All surgeries in both groups were performed by the same surgeons (H. Z, T. B, and H. W).

In the navigation group, a digital reference frame was fixed to the patient's forehead using screws inserted through small incisions in the scalp (Fig. 2A). The surgeon registered a series of points on the face using the CT dataset to match the actual maxillofacial skeleton and the navigation images. During surgery, the fractured bones were elevated into their proper positions, which were confirmed using the mirror images and the navigation probe (Fig. 2B). In this way, reduction was conducted following the

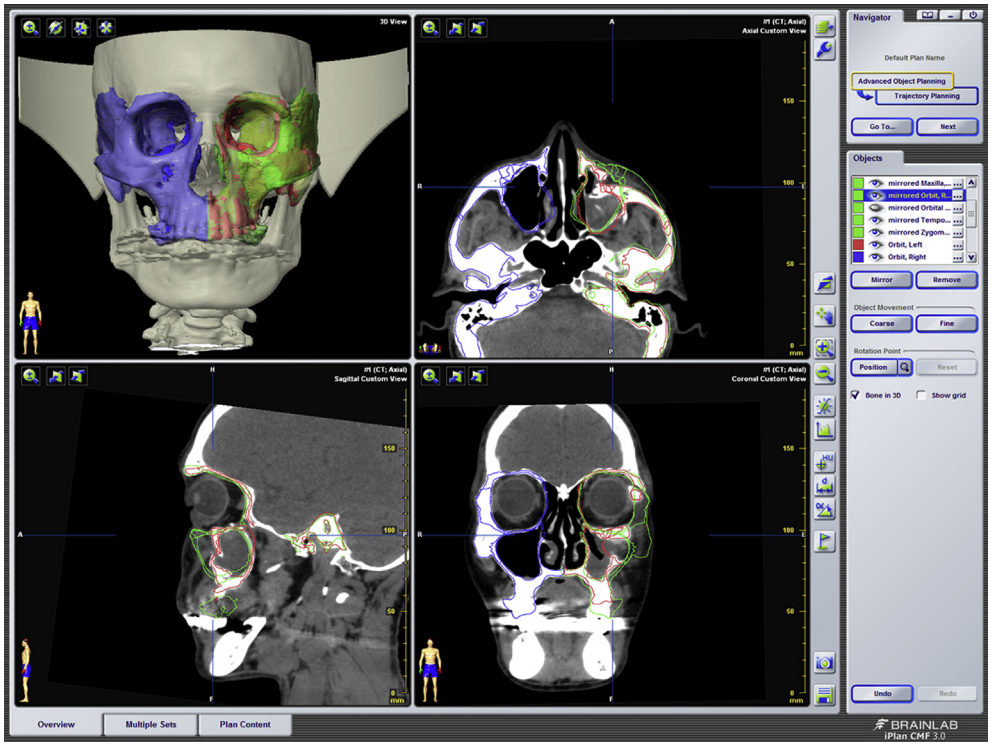

Fig. 1. Mirror image of the healthy side (blue), used to create a virtual plan (green) for the affected side (red).

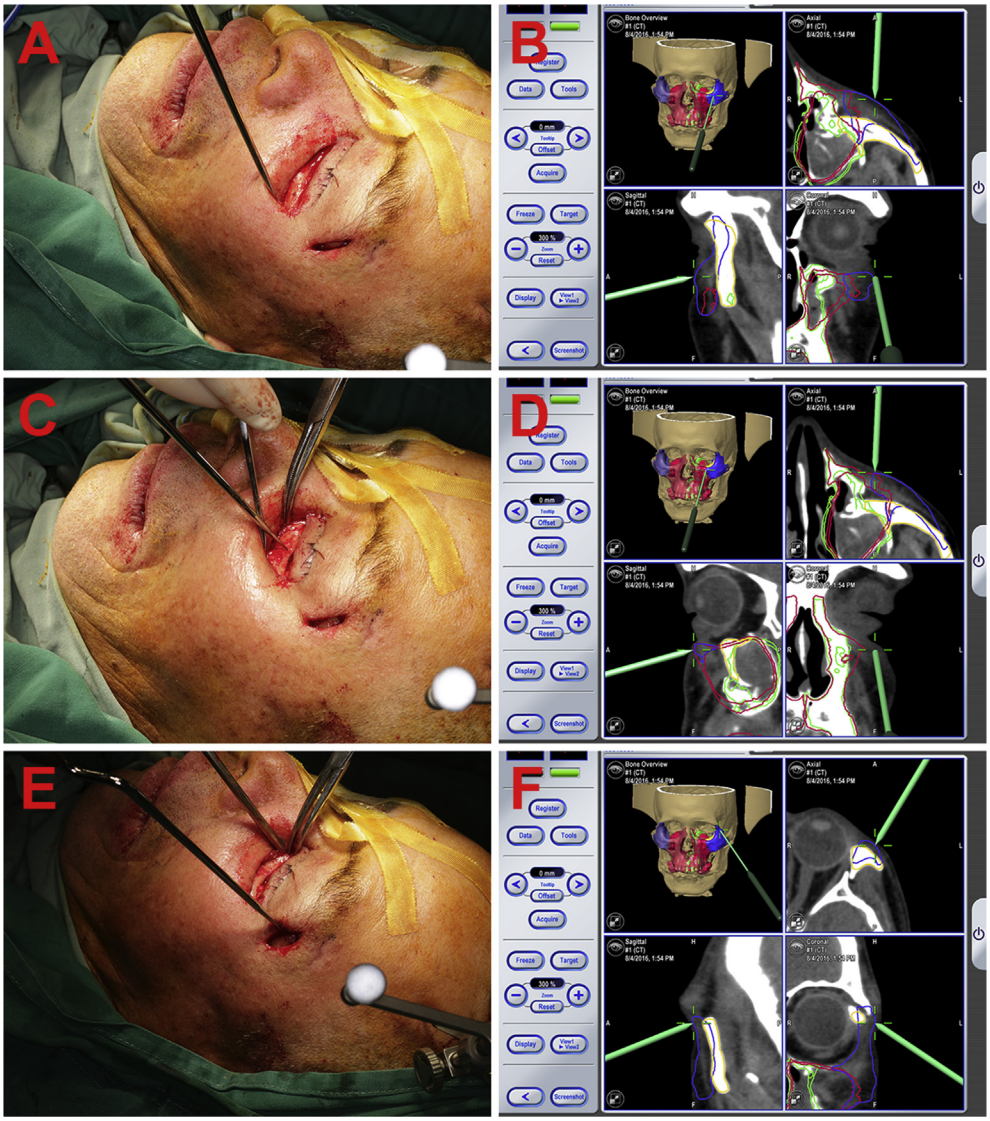

Fig. 2. Application of surgical navigation to zygomaticomaxillary complex (ZMC) fracture reduction. (A, C, E) A probe was used intraoperatively to verify the positions of the maxillozygion (MZ), orbitale (O), and suprajugal curvature (SJC). (B, D, F) The navigation tracked MZ, O, and SJC.

planned contour line. Then, the fractures were fixed using titanium plates and screws (Synthes, Zuchwil, Switzerland).

The computer-assisted design procedure used for the control group was similar to that used for the navigation group, but the virtual mirrored models were used only for postoperative analysis. The operations in the control group were performed without surgical navigation, and surgeons judged facial symmetry visually. If any discrepancy occurred, the surgeons would discuss and adjust the position of bone to achieve an outcome that was acceptable for every surgeon.

2.3. Outcome analysis

All patients were followed up in the 2nd week, 3rd month, 6th month, 12th month and 18th month postoperatively. A postoperative CT scan was performed in the 2nd week on every patient after surgery.

2.3.1. Chromatography

The preoperative and postoperative CT images and digital models of the navigation plan were outputted as stereolithographic (STL) files, and then imported into Geomagic Studio 14.0 (Geomagic, Morrisville, NC, USA). The three models were superimposed with alignment of nonsurgical portions. A color-graded error map was generated to show the deviation between corresponding points on the postoperative CT and virtual planning models (Fig. 3).

2.3.2. ZMC asymmetry index

Before measurement, five pairs of zygomatic landmarks were selected for quantitative analysis (Table 1). Two investigators (T. B and D. Y) manually identified all landmarks. The positions of the landmarks were confirmed using a three-dimensional (3D) multiplanar view.

For the symmetry analysis, a 3D coordinate system was constructed (Fig. 4). The *x* axis, determined first, included nasion (N) and extended between the right and left orbitales. The *y* axis included N and extended perpendicular to the *x* axis in the FH plane. The *z* axis included N and was perpendicular to the *x* and *y* axes. The common origin (0, 0, 0) of the three axes was N. The median sagittal plane, delineated in previous steps, served as the sagittal plane (YZ). The transverse plane (XZ) was defined as parallel to the FH plane and passing through N. The coronal plane (XY)

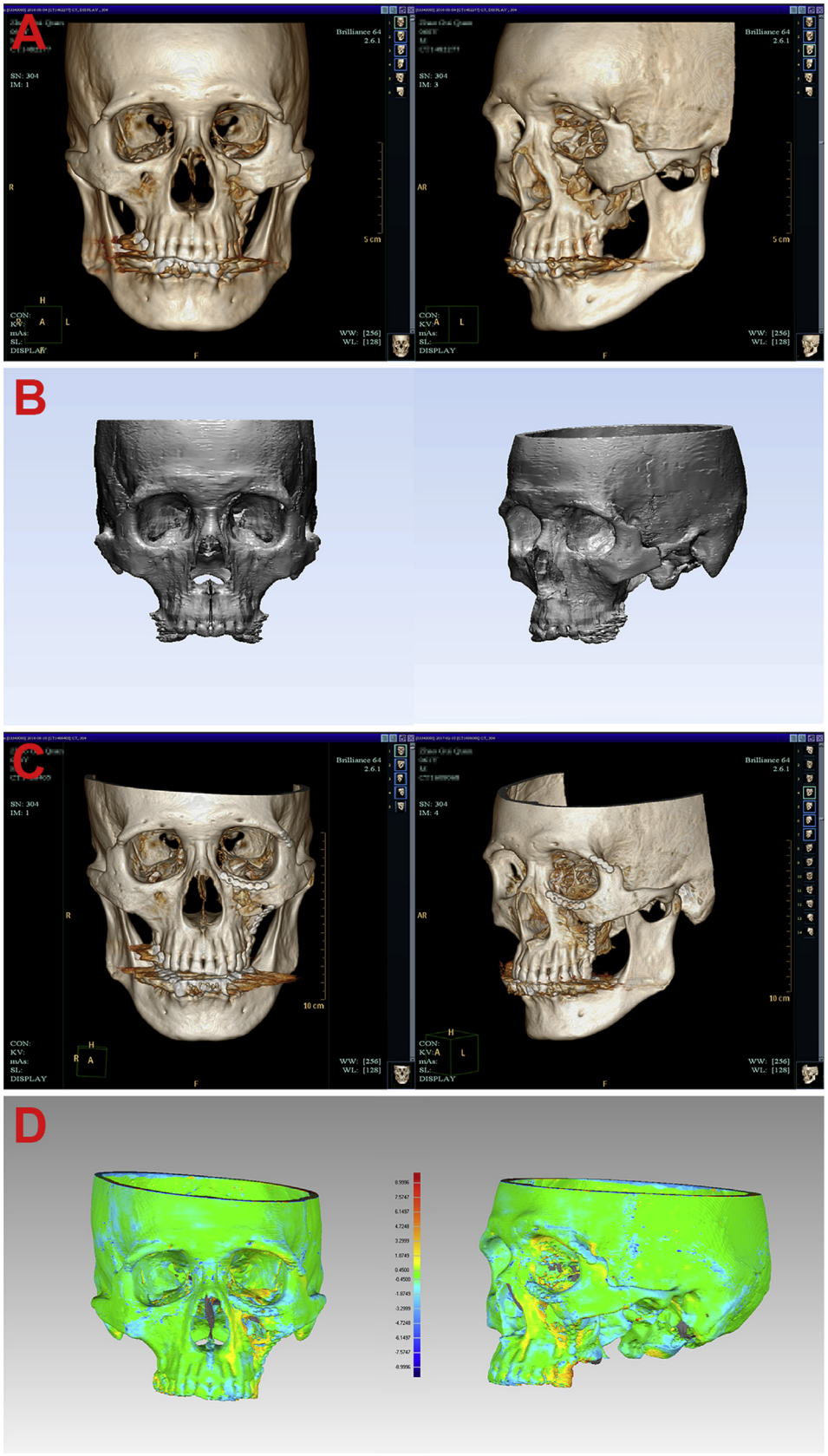

Fig. 3. The outcome of navigation-assisted ZMC reduction. (A) Preoperative three-dimensional (3D) computed tomography (CT) of ZMC fracture. (B) Virtual plan made by mirroring of the healthy contralateral ZMC. (C) Postoperative 3D CT. (D) Chromatographic analysis of the virtual plan and postoperative CT image.

Table 1
Landmarks selected for ZMC symmetry analysis.

Landmark	Abbreviation	Description
Orbitale	O	Most inferior point of the infraorbital rim
Maxillozygion	MZ	Most anterior point on the maxillozygion suture line below the lateral third of the orbit
Suprajugal curvature	SJC	Most convex point of the posterior edge of the frontal process of the zygomatic bone superior to jugale
Jugale	J	Most concave point between the lateral margin of the frontal process and the upper margin of the temporal process of the zygomatic bone
Zygion	Z	Most lateral point on the zygomatic arch

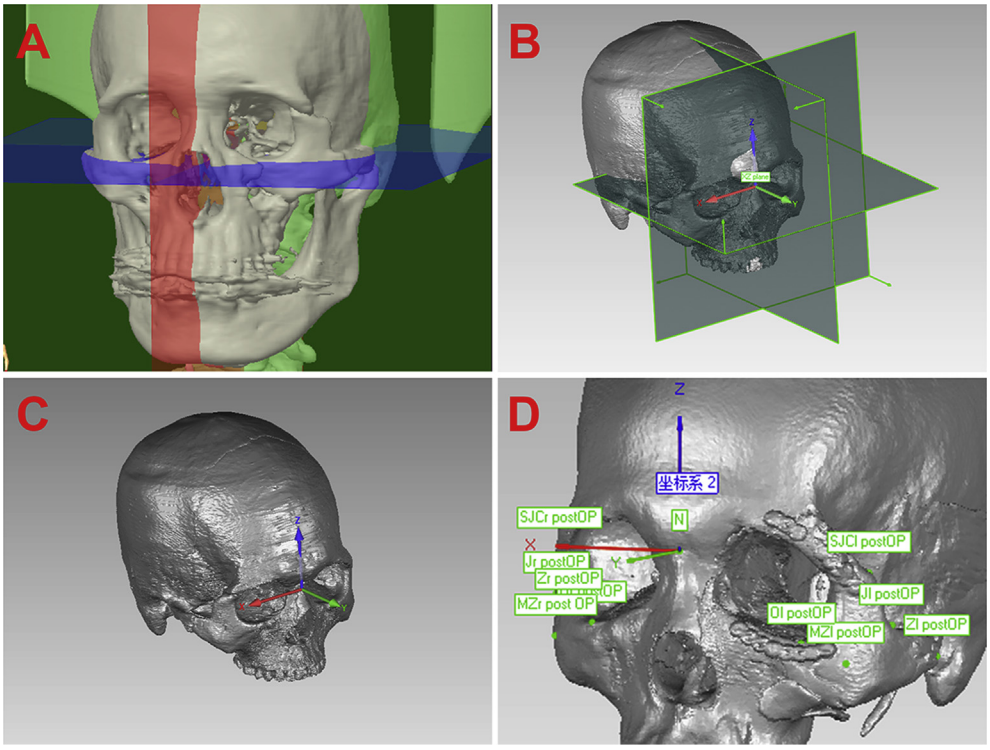

Fig. 4. Establishment of the coordinate system and identification of landmarks. (A) The median sagittal plane (red) and Frankfort horizontal (FH) plane (blue). (B) The sagittal plane (YZ) plane was determined as the median sagittal plane, the transverse plane (XZ) plane was defined parallel to the FH plane and passing through nasion (N), and the coronal plane (XY) plane was perpendicular to YZ and XZ. (C) The coordinate system. (D) Identification of five pairs of landmarks.

was defined as perpendicular to YZ and XZ. The three planes met at N, which was taken to be the origin of the coordinate system.

The X, Y, and Z coordinates of the landmarks in their confirmed final positions were recorded (Fig. 5). According to Huang et al. (2013), the asymmetry index (AI) was calculated as follows:

$$\mathrm{AI} = \sqrt{(Xl + Xr)^2 + (Yl - Yr)^2 + (Zl - Zr)^2}$$

where *X*, *Y*, and *Z* are the coordinates of a landmark; *l* stands for left and *r* stands for right. A perfectly symmetrical landmark has an AI of 0. Increasing AI values indicate increasing degrees of asymmetry. The average AI for each of the five landmarks was calculated for each group. Because of the use of an absolute value, the AI does not describe the direction in which individual parts of the face deviate from symmetry.

2.3.3. Orbital volume

Preoperative CT data revealed orbital volume changes in 21 of the 25 cases (11 in the navigation group, 10 in the control group). Using iPlan 3.0 software and CT data in DICOM format, the orbital cavities were auto-segmented (Fig. 6A,B). When an orbital interface was not identified due to orbital wall defects at the fracture site, the orbital volume was measured using the soft tissue interface. STL data for the orbital cavities were imported into 3-matic Research 9.0 software (×64; Materialize NV, Leuven, Belgium), and the orbital volume was subsequently measured (Fig. 6C,D).

Volumes of the uninjured orbits were measured automatically and recorded as the target (normal) volumes (V_{normal}s). The volumes of fractured orbits were calculated before and after surgery and recorded as the fractured orbital volumes (V_{preop}s) and reconstructed orbital volumes (V_{postop}s), respectively.

The recovery ratio (RR) for orbital volume was calculated using the following formula:

$$\mathrm{RR} = \frac{Vpostop}{Vnomal} \times 100\%$$

The amount of reduction (reduced volume [RV]) was calculated using the formula $RV = Vpostop - Vpreop$.

The results were analyzed statistically using SPSS software (ver. 19.0; SPSS Inc., Chicago, IL, USA). The *t* test was used to compare means between groups, and the paired *t* test was used to assess the

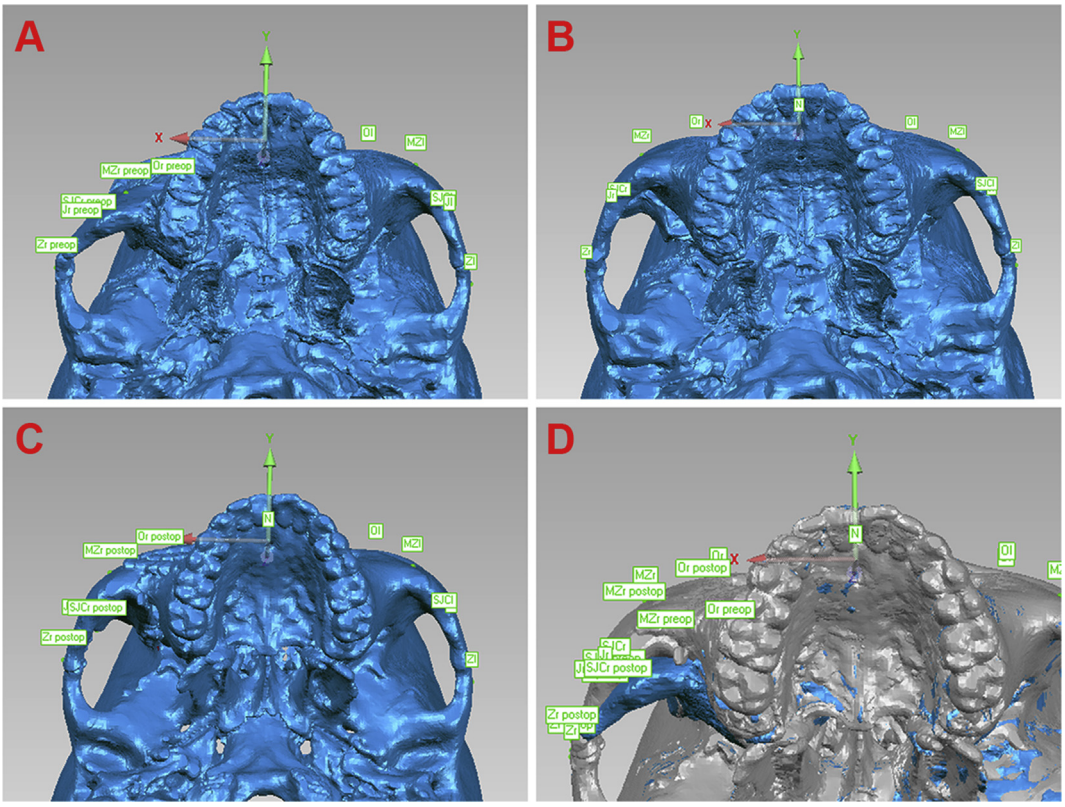

Fig. 5. Bottom views of the landmarks on stereolithographic (STL) files used to record X, Y, and Z coordinates. (A) Landmarks on a preoperative STL file. (B) Landmarks on an STL file of the virtual plan. (C) Landmarks on a postoperative STL file. (D) Comparison of landmarks among the three STL files.

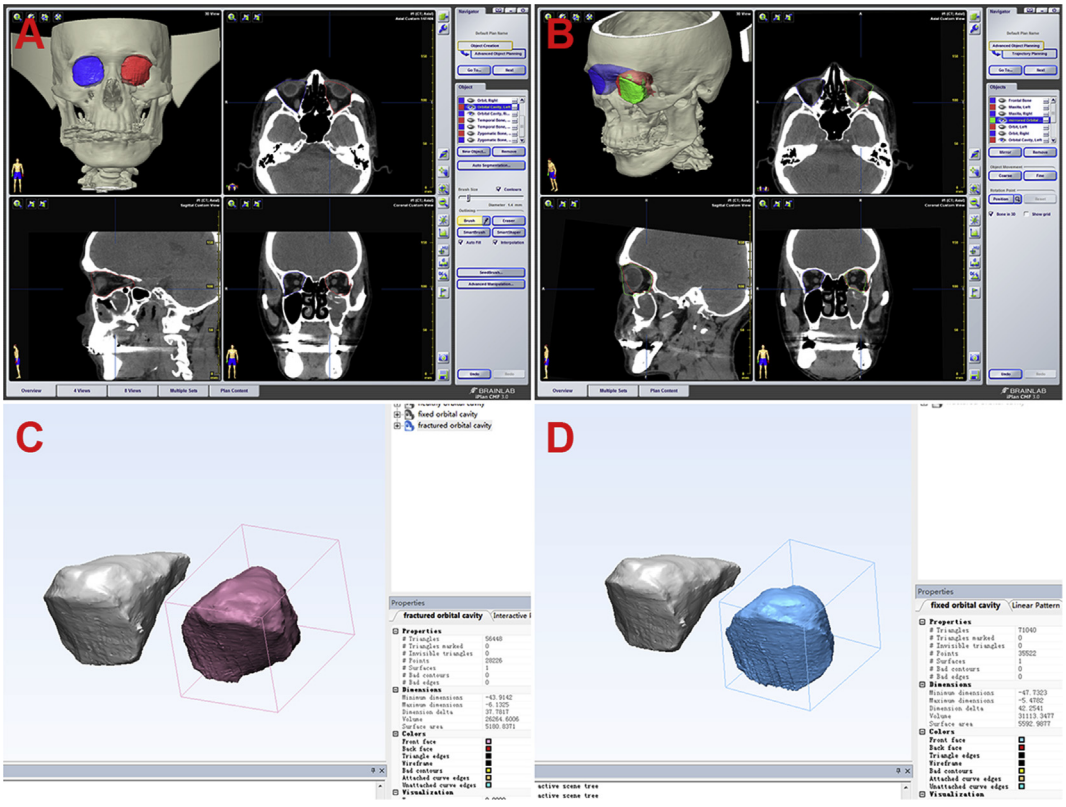

Fig. 6. Calculation of orbital volumes. (A) Identification of the fractured (red) and healthy (blue) orbital cavity models. (B) Identification of the mirrored model (green) from the healthy orbital cavity. (C) STL files of the normal and fractured orbital cavities were imported into 3-Matic for volume measurement. (D) Measurement of the reconstructed orbital cavity volume.

efficacy of ZMC symmetry and orbital volume restoration in each group. *P* values < 0.05 were considered significant.

3. Results

All 25 patients recovered uneventfully after the operations. During follow-up, no mucosal or cutaneous plate exposure was observed in any patient. Five patients (three in the navigation group, two in the control group) complained of temporary facial nerve injury, which resolved within 6 months. Three patients in the control group complained of facial asymmetry in the zygion (Z) area, but refused surgical revision. No patient experienced a postoperative orbital complication, such as extraocular movement dysfunction, diplopia, or enophthalmos.

Chromatography was used to compare the postoperative CT and virtual mirrored models. Superimposition of the planned and postoperative skull configurations revealed a high degree of similarity between the reduced ZMCs and the surgical plans in the navigation group (Fig. 3D).

The preoperative AIs for the five pairs of landmarks did not differ significantly between groups. Postoperatively, the AIs for orbitale (O), maxillozygion (MZ), and Z in both groups, and the AI for jugale (J) in the navigation group, had decreased significantly ($p < 0.01$); the AIs for J in the control group and the suprajugal curvature in both groups showed no significant reduction. In addition, the postoperative AIs for three landmarks were significantly lower in the navigation group than in the control group (O: 3.43 ± 0.47 [range: 2.41–4.08] vs. 4.86 ± 0.86 [range: 3.65–6.3]; J: 4.20 ± 0.83 [range: 3.27–6.22] vs. 4.86 ± 0.86 [range: 5.31–7.38]; Z: 4.92 ± 1.53 [range: 2.38–7.64] vs. 10.04 ± 3.04 [range: 4.15–12.74]; all $p < 0.01$) (Table 2).

The mean volume of the unfractured orbit was 26.91 ± 1.46 cm^3 (range: 24.29–28.92 cm^3) in the navigation group and 26.3 ± 1.56 cm^3 (range: 24.18–29.11 cm^3) in the control group ($p = 0.362$). The mean volume of the fractured orbit was 24.92 ± 1.24 cm^3 (range: 22.94–26.56 cm^3) in the navigation group and 24.41 ± 1.99 cm^3 (range: 21.14–28.80 cm^3) in the control group ($p = 0.485$). The mean reconstructed orbital volume was 27.07 ± 2.21 cm^3 (range: 23.50–31.11 cm^3) in the navigation group and 26.01 ± 2.22 cm^3 (range: 23.10–30.43 cm^3) in the control group ($p = 0.287$). The mean RR was 100.49% ± 3.74% (range: 96.03–107.60%) in the navigation group and 98.79% ± 3.21% (range: 95.49–104.55%) in the control group ($p = 0.281$). The RV differed significantly between the navigation and control groups (2.15 ± 1.4 cm^3 [range: 0.56–4.85 cm^3] vs. 1.6 ± 0.64 cm^3 [range: 0.84–2.26 cm^3]; $p = 0.011$) (Table 3).

4. Discussion

Facial bones are relatively symmetrical, contributing to facial aesthetics. Differences >3 mm between bilateral bones are deemed unacceptable (Chu et al., 2011). Therefore, the global criteria for ZMC reduction focus primarily on the recovery of symmetry. In early studies, the postoperative degree of ZMC symmetry was judged visually and subjectively. In recent decades, various techniques for accurate facial asymmetry quantification have been developed. Most of these techniques are based on the analysis of deviation using distances between bilateral landmarks (Verhoeven et al., 2016; Gong et al., 2014). Landmark-based symmetry scoring is commonly used for bones and soft tissues (Belcastro et al., 2016; Alqattan et al., 2015), and its accuracy and reproducibility have been examined thoroughly.

As pre-traumatic photographs are typically unavailable for comparison, the ideal shape and position of an injured ZMC can be determined with reference to the uninjured side, especially in the case of comminuted fracture. Before surgery, a mirrored virtual model can be used to define the target reduction. The key point in the construction of a sensible mirrored model is the identification of a reasonable midsagittal reference plane (Furst et al., 2001). Any three midpoints, which include N, the apex nasi, the sella, the anterior nasal spine, the posterior nasal spine, and pogonion, can be used to form the plane (Shin et al., 2016; Kim et al., 2014a). Unfortunately, these midpoints may be affected by developmental deformities or destroyed by fracture. In this study, the midsagittal

Table 2
Pre- and postoperative AIs for five pairs of landmarks.

AI		Preoperative	Postoperative	*p* (pre. vs. post.)
O	Navigation group	11.09 ± 1.50	3.43 ± 0.47	<0.01*
	Control group	11 ± 1.29	4.86 ± 0.86	<0.01*
	p	0.88	<0.01*	
MZ	Navigation group	13.79 ± 2.00	6.57 ± 0.94	<0.01*
	Control group	14.90 ± 1.66	6.28 ± 0.82	<0.01*
	p	0.16	0.45	
SJC	Navigation group	4.53 ± 0.93	4.73 ± 0.74	0.59
	Control group	5.21 ± 0.85	5.05 ± 1.04	0.72
	p	0.08	0.38	
J	Navigation group	6.48 ± 1.37	4.20 ± 0.83	<0.01*
	Control group	6.68 ± 1.24	6.47 ± 0.84	0.66
	p	0.71	<0.01*	
Z	Navigation group	10.33 ± 3.63	4.92 ± 1.53	<0.01*
	Control group	12.78 ± 2.80	10.04 ± 3.04	<0.01*
	p	0.08	<0.01*	

*$p < 0.05$.

Table 3
Analysis of orbital volumes.

Group	Normal orbital volume (cm^3)	Fractured orbital volume (cm^3)	Reconstructed orbital volume (cm^3)	Reduced volume (cm^3)	Recovery ratio (%)
Navigation group	26.91 ± 1.46	24.92 ± 1.24	27.07 ± 2.21	2.15 ± 1.4	100.49 ± 3.74
Control group	26.3 ± 1.56	24.41 ± 1.99	26.01 ± 2.22	1.6 ± 0.64	98.79 ± 3.21
p	0.362	0.485	0.287	<0.01*	0.281

*$p < 0.05$.

plane was defined to pass through N and the midpoint of the sella turcica on frontal views, and was oriented perpendicular to the FH plane. This method avoided prominent points on the face to decrease the influence from the trauma, and made use of the stability of the FH plane. This has been proved to be clinically applicable in most people (Gateno et al., 2016) and 3D coordinate systems established on the basis of these planes have been reported to be reliable and reproducible (Lonic et al., 2017; Kim et al., 2014b).

Another challenge is the identification of the exact positions of landmarks on tomographic images, as landmark locations appear different on different views. In this study, we chose five pairs of landmarks having stable relationships with anatomic sutures or points on the zygoma. We believe that this approach increased the ease of identification and minimized error (Belcastro et al., 2016). Moreover, two observers performed each identification independently before discussing the findings and resolving discrepancies. These landmarks are distributed across the surface of the zygomatic bone and represent the most likely ZMC fracture and displacement regions, involving the orbital cavity, zygomatic arch, and zygomatic eminence. We believe that the wide distribution of these ZMC landmarks improves the ability to evaluate symmetry, reflecting the accuracy of reduction in different areas.

The comparison of pre- and postoperative AIs revealed the results of surgery in the two groups. Surgery (with or without navigation) significantly decreased the AIs for most points on the ZMC surface, indicating an effective increase in symmetry. Moreover, significant differences in symmetry recovery between groups were evident around the infraorbital rim, zygomatic arch, and posterior bony margin of the orbit. Facial width and aesthetics are linked directly to symmetry in these areas. These findings prove that the use of computer navigation can improve facial symmetry when aligning fractured bones. The results of chromatographic analysis also support this conclusion. The AI for MZ, which represents the zygomatic prominence, did not differ between two groups. The exact reason for this lack of difference is unknown, but it may be attributed to the lack of intraoperative exposure of MZ. In this study, local mini-incisions were used to expose the fractures in both groups to minimize scarring, which allowed direct visualization of all landmarks except MZ. This approach rendered accurate reduction of MZ difficult. To solve this problem, we recommend more effective exposure of the ZMC, such as by coronal incision.

ZMC fractures are usually associated with changes in orbital cavity volume (Sharma et al., 2016). We argue that a full assessment of ZMC reduction must include measurement of the orbital volume. The orbital measurement method used in this study has been proved to be reliable and reproducible (Tahernia et al., 2009; Gordon et al., 2012; Liu et al., 2013). No significant difference in the postoperative orbital cavity volume was observed between groups, implying that the orbital volume on the injured side was corrected to a similar degree by surgery with and without navigation. On the other hand, the RV differed significantly between groups, reflecting a greater degree of restoration in the navigation group. However, the cases included in this study represent a small proportion of ZMC fracture cases. Given their potential impedance of virtual navigation planning, naso-orbito-ethmoidal fractures were excluded. Thus, our orbital volume findings do not represent the results obtained for more severe orbital fractures, which should be studied in future works.

In ZMC fracture cases, consideration must be given to medical and other aspects. The use of navigation increases the operative time by about 1 h. Nevertheless, a CANS can be used to avoid repeated alignment of the fractured bones. We believe that the time spent on actual navigation during surgery is more or less compensated by the time saved due to better orientation and more rapid evaluation of accuracy. Therefore, CANS use has been recommended for most zygomatic fractures (He et al., 2013; Li et al., 2015). On the other hand, the preparation of a patient for navigation involves additional effort on the part of the patient and the surgeon. The design of plans usually takes approximately 2 h. However, no extra cost was associated with navigation use for any patient in our study. Our institution currently applies no additional charge for navigation and planning.

The primary limitation of this study was its retrospective nature. Another weakness was selection bias, where the patients were not randomized to the two groups, which inherently reduced the capacity for comparison. Future prospective trials comparing these techniques are warranted.

5. Conclusion

In conclusion, the application of a surgical navigation system to ZMC fracture reduction had the advantages of greater predictability and effectiveness, improving the symmetry of the bilateral ZMC. Our quantitative assessment successfully reflected symmetry levels and statistical differences.

Funding

This work was supported by the National Natural Science Foundation of China (Grant Number: 31570989), the Natural Science Foundation of Zhejiang Province, China (Grant Number: LY15H140002) and the Medical & Health Scientific Project of Zhejiang Province, China (Grant Number: 2019RC154, 2017ky328).

Declarations of interest

None.

Appendix A. Supplementary data

Supplementary data to this article can be found online at https://doi.org/10.1016/j.jcms.2018.12.003.

References

Alqattan M, Djordjevic J, Zhurov AI, Richmond S: Comparison between landmark and surface-based three-dimensional analyses of facial asymmetry in adults. Eur J Orthod 37: 1–12, 2015

Belcastro A, Willing R, Jenkyn T, Johnson M, Galil K, Yazdani A: A three-dimensional analysis of zygomatic symmetry in normal, uninjured faces. J Craniofac Surg 27: 504–508, 2016

Bogusiak K, Arkuszewski P: Characteristics and epidemiology of zygomaticomaxillary complex fractures. J Craniofac Surg 21: 1018–1023, 2010

Chu EA, Farrag TY, Ishii LE, Byrne PJ: Threshold of visual perception of facial asymmetry in a facial paralysis model. Arch Facial Plast Surg 13: 14–19, 2011

Furst IM, Austin P, Pharoah M, Mahoney J: The use of computed tomography to define zygomatic complex position. J Oral Maxillofac Surg 59: 647–654, 2001

Gateno J, Jajoo A, Nicol M, Xia JJ: The primal sagittal plane of the head: a new concept. Int J Oral Maxillofac Surg 45: 399–405, 2016

Gong X, He Y, He Y, An JG, Yang Y, Zhang Y: Quantitation of zygomatic complex symmetry using 3-dimensional computed tomography. J Oral Maxillofac Surg 72: 2053, 2014 e1–e8

Gordon CR, Susarla SM, Yaremchuk MJ: Quantitative assessment of medial orbit fracture repair using computer-designed anatomical plates. Plast Reconstr Surg 130: 698e–705e, 2012

He Y, Zhang Y, An JG, Gong X, Feng ZQ, Guo CB: Zygomatic surface marker-assisted surgical navigation: a new computer-assisted navigation method for accurate treatment of delayed zygomatic fractures. J Oral Maxillofac Surg 71: 2101–2114, 2013

Huang CS, Liu XQ, Chen YR: Facial asymmetry index in normal young adults. Orthod Craniofac Res 16: 97–104, 2013

Kim JY, Jung HD, Jung YS, Hwang CJ, Park HS: A simple classification of facial asymmetry by TML system. J Craniomaxillofac Surg 42: 313–320, 2014a

Kim DH, Kim RH, Lee J, Chee YD, Kwon KH: Evaluation of soft tissue asymmetry using cone-beam computed tomography after open reduction and internal fixation of zygomaticomaxillary complex fracture. J Korean Assoc Oral Maxillofac Surg 40: 103–110, 2014b

Lerhe B, Alshehri S, Ferachon D, Dejean S, Salabert AS, Lopez R: Tomographic osteometry of the zygomatic bone applied to traumatology of facial bones:

preliminary retrospective study of zygomatic summit in 28 patients. J Craniomaxillofac Surg 45: 150–156, 2017
Li Z, Yang RT, Li ZB: Applications of computer-assisted navigation for the minimally invasive reduction of isolated zygomatic arch fractures. J Oral Maxillofac Surg 73: 1778–1789, 2015
Liu XZ, Shu DL, Ran W, Guo B, Liao X: Digital surgical templates for managing high-energy zygomaticomaxillary complex injuries associated with orbital volume change: a quantitative assessment. J Oral Maxillofac Surg 71: 1712–1723, 2013
Lonic D, Sundoro A, Lin HH, Lin PJ, Lo LJ: Selection of a horizontal reference plane in 3D evaluation: identifying facial asymmetry and occlusal cant in orthognathic surgery planning. Sci Rep 7: 2157, 2017
Lübbers HT, Jacobsen C, Matthews F, Grätz KW, Kruse A, Obwegeser JA: Surgical navigation in craniomaxillofacial surgery: expensive toy or useful tool? A classification of different indications. J Oral Maxillofac Surg 69: 300–308, 2011
Marinho RO, Freire-Maia B: Management of fractures of the zygomaticomaxillary complex. Facial Plast Surg Clin North Am 25: 617–636, 2013
Ozyazgan I, Günay GK, Eskitaşçioglu T, Ozköse M, Coruh A: A new proposal of classification of zygomatic arch fractures. J Oral Maxillofac Surg 65: 462–469, 2007
Salentijn EG, van den Bergh B, Forouzanfar T: A ten-year analysis of midfacial fractures. J Craniomaxillofac Surg 41: 630–636, 2013
Sharma R, Muralidharan CG, Roy ID, Jain NK, Patrikar S: Radiological evaluation of sphenozygomatic suture fixation for restoration of orbital volume: a retrospective study. J Craniomaxillofac Surg 44: 1903–1908, 2016
Shin SM, Kim YM, Kim NR, Choi YS, Park SB, Kim YI: Statistical shape analysis-based determination of optimal midsagittal reference plane for evaluation of facial asymmetry. Am J Orthod Dentofacial Orthop 150: 252–260, 2016
Tahernia A, Erdmann D, Follmar K, Mukundan S, Grimes J, Marcus JR: Clinical implications of orbital volume change in the management of isolated and zygomaticomaxillary complex–associated orbital floor injuries. Plast Reconstr Surg 123: 968–975, 2009
Verhoeven T, Xi T, Schreurs R, Bergé S, Maal T: Quantification of facial asymmetry: a comparative study of landmark-based and surface-based registrations. J Craniomaxillofac Surg 44: 1131–1136, 2016